Available online at www.sciencedirect.com
ScienceDirect
Trans. Nonferrous Met. Soc. China 28(2018) 766−774
Transactions of Nonferrous Metals Society of China
www.tnmsc.cn

Bio-dissolution of pyrite by *Phanerochaete chrysosporium*

Hong-ying YANG[1], Qian LIU[1,2], Guo-bao CHEN[1], Lin-lin TONG[1], Auwalu ALI[1]

1. School of Metallurgy, Northeastern University, Shenyang 110819, China;
2. Shanghai Collaborative Innovation Centre for WEEE Recycling, Shanghai Polytechnic University, Shanghai 201209, China

Received 29 December 2016; accepted 28 October 2017

Abstract: The dissolution of pyrite was studied with *Phanerochaete chrysosporium* (*P. chrysosporium*). This fungus resulted in the dissolution of 18% iron and 33% sulfur. The oxidization layer was formed on the pyrite surface, which probably consisted of iron oxide, iron oxy-hydroxide, iron sulfate, elemental sulfur and mycelia. The electrochemical characteristics of pyrite were studied in the systems without and with *P. chrysosporium*. *P. chrysosporium* could accelerate the dissolution of pyrite by decreasing pitting potential and polarization resistance plus improving polarization current, corrosion potential and corrosion current density. The dissolution of pyrite is the combined effect of enzymes, hydrogen peroxide, ferric iron and organic acids. Enzymes attack the chemical bonds by free radicals. Organic acids dissolve pyrite by acidolysis and complexolysis. Enzymes and hydrogen peroxide play an essential role in this process.

Key words: *Phanerochaete chrysosporium*; pyrite; bio-dissolution; Carlin-type gold ores; electrochemistry

1 Introduction

Carlin-type gold ores are a kind of refractory gold ores due to the micro-disseminated gold and the "preg-robbing" of carbonaceous compounds. Gold is frequently hosted in sulfide minerals in the form of micro or sub-micro particles, which inhibits the contact of gold and the leaching solution. Furthermore, the gold-bearing sulfides have the "preg-robbing" capacity due to the presence of active sites which can adsorb and reduce gold [1−3]. Therefore, the dissolution of sulfide minerals is required to open the gold inclusion and reduce the "preg-robbing" capacity. Bio-oxidation has received much attention because of the advantages such as mild conditions, selective oxidation and environmental friendliness.

The leaching of gold-bearing sulfides were successfully achieved by *Acidithiobacillus ferrooxidans*, *Acidithiobacillus thiooxidans* and *Leptospirillum ferrooxidans*. The bio-leaching mechanism of sulfide minerals is determined by the minerals structure. The intermediate thiosulfate plays an important role in the dissolution of pyrite [4]. YANG et al [5] discovered that the crystal structure and the arsenic valence played an important role in the bio-leaching process. But the lithotrophic bacteria are unable to oxidize and deactivate carbonaceous matter [6,7]. Moreover, carbonaceous matter was activated in the bacterial leaching stage due to the required acidic environment [8]. Recently, researches have been focused on the two-stage biological pretreatment process. In this process sulfide minerals were oxidized by the lithotrophic bacteria firstly, and then carbonaceous matter was deactivated and degraded by heterotrophic microorganisms such as *Streptomyces setonii*, *Trametes versicolor* or *Pseudomonas* sp. [7,9]. However, this process has many disadvantages such as the cohesion difficulty between autotrophic and heterotrophic microbial processes. Presently, only a few studies have been performed using fungi to decompose sulfide minerals. Some of fungi have the capacity to leach metals from various materials. *Aspergillus niger* can leach various metals from sulfide ores, fly ash, red mud and lateritic chromite overburden using excreted organic acids such as citric acid, oxalic acid and gluconic acid [10−13]. DENG et al [14] found that *Penicillium*

Foundation item: Project (U1608254) supported by the National Natural Science Foundation of China
Corresponding author: Hong-ying YANG; Tel: +86-24-83680373; E-mail: yanghy@smm.neu.edu.cn
DOI: 10.1016/S1003-6326(18)64709-0

chrysogenum F1 could effectively remove heavy metals from polluted soil and smeltery slag by the generated organic acids. OFORI-SARPONG et al [6] decomposed pyrite and arsenopyrite using *P. chrysosporium*. After 21d of fungal treatment, the degradation amount of pyrite and arsenopyrite reached 15% and 35%, respectively.

P. chrysosporium has many advantages such as extracellular lignin degradation system, non-inducible enzymes, diversity of substrates and antagonism to other microorganisms. As a response to nutrient limitation, *P. chrysosporium* can synthesize and secrete a multitude of enzymes such as laccase (Lac), lignin peroxidase (LiP) and manganese peroxidase (MnP). These enzymes can contribute to degrade sulfide minerals [15]. *P. chrysosporium* can not only degrade carbonaceous materials [16,17], but also remove sulfide minerals from coals and gold ores [6,18,19]. Therefore, *P. chrysosporium* is considered as a potentially usable fungus for pretreating refractory gold ores. Pyrite is the most important gold-bearing mineral. The oxidation activity of pyrite is the weakest in the bio-oxidation sequence of sulfide minerals. Therefore, this study is to develop and improve the dissolution of pyrite by *P. chrysosporium*. The change of the important experimental factors and the electrochemical behavior of pyrite without and with fungi are systematically studied. This study provides the possibility of removing the disadvantages of the two-stage bio-oxidation process by the simultaneous treatment of sulfide minerals and carbonaceous matter in Carlin-type gold ores.

2 Experimental

2.1 Materials

The pyrite sample was collected from a Shaanxi gold ore in China. The contents of iron, sulfur, arsenic, nickel, copper and cobalt are 44.89%, 51.37%, 0.58%, 0.24%, 0.16% and 0.39%, respectively. After fine grinding in ball mills, the particle size of pyrite reached 89% of less than 75 μm. *P. chrysosporium* (CCTCC M 2013616) was obtained from China Center for Type Culture Collection. The nitrogen limited medium was selected, since the excessive nitrogen supply could inhibit the formation of the ligninolytic enzyme system [20]. The nitrogen limited medium contains 10 g/L glucose, 0.20 g/L KH_2PO_4, 1 g/L $MgSO_4·7H_2O$, 0.37 g/L ammonium tartrate, 0.02 g/L $CaCl_2$, 1 mg/L thiamin-HCl and 70 mL/L trace element solution. The trace element solution is composed of 0.586 g/L glycine, 1 g/L NaCl, 0.10 g/L $CoSO_4$, 0.01 g/L $CuSO_4·5H_2O$, 0.01 g/L Na_2MoO_4, 0.01 g/L H_3BO_3, 0.01 g/L $KAl(SO_4)_2·12H_2O$, 0.10 g/L $ZnSO_4·7H_2O$, 0.082 g/L $CaCl_2$, 0.10 g/L $FeSO_4·7H_2O$, 3 g/L $MgSO_4·7H_2O$ and 0.50 g/L $MnSO_4·7H_2O$.

2.2 Bio-dissolution of pyrite

The fungal dissolution experiments of pyrite were performed in 500 mL Erlenmeyer flasks containing 200 mL medium. Firstly, the media and pyrite samples were autoclave-sterilized at 121 °C for 20 min. The number of spores was counted by a blood counting chamber and the concentration was adjusted to approximately 3×10^5 spores per mL. Then, 0.50 mL spore suspensions per flask were incubated in medium with the sterilized pyrite. The fungal dissolution experiments were conducted at 30 °C, pulp density 5% and 150 r/min shaking culture for 24 d. The nitrogen limited medium without fungi was used for the parallel control experiment in order to evaluate the effect of medium to pyrite dissolution. The control experiment was performed under sterile and anaerobic conditions. The growth of *P. chrysosporium* was also investigated in the nitrogen limited medium without pyrite. The initial pH was 5 in the experimental and control assays. Each test was performed in triplicate to check reproducibility. 5 mL samples were aseptically withdrawn every 4 d to measure the concentration of iron ions, sulfate ions, organic acids and enzymes as well as pH and redox potential (E_h). The loss of medium due to sampling was compensated with the fresh sterilized medium. The samples were filtered and washed with deionized water at the end of experiments. The dry mass of the fungal biomass was also determined.

2.3 Assay of enzyme activity

2 mL samples were centrifuged at 7500 *g* for 15 min. The supernatant was collected and used for the enzyme activity assay. Control experiments were carried out with heat-inactivated enzymes. The activities of LiP, MnP and Lac were measured to evaluate their roles in the dissolution of pyrite. LiP activity was evaluated by the absorbance change of the reaction liquid within 2 min at 310 nm. One unit of enzyme activity is defined as the required enzyme amount that transforms 1 μmol substrate per minute [21]. MnP activity was determined by the absorbance change of the reaction liquid for 2 min at 240 nm. The amount of enzyme, oxidizing 1mmol Mn^{2+} to Mn^{3+} in 1 min, is taken as one unit of enzyme activity [22]. Lac activity was measured by the guaiacol method. One unit of enzyme activity is defined as the required enzyme amount which receives an increase of 0.01 unit of absorbance per minute at 465 nm [23].

2.4 Electrochemical experiments

The electrochemical experiments were performed using a three-electrode electrolytic cell with pyrite as the working electrode and the platinum as the counter-electrode. A saturated standard calomel electrode (SCE) was used as the reference electrode. The electrolyte was

the nitrogen limited medium with and without *P. chrysosporium*. All experiments were conducted at 30 °C. At first, open circuit potential (OCP) of sample was measured. The steady-state of system was defined as the OCP change of less than 2 mV (vs SCE) per minute. Subsequently, the steady-state polarization curve of sample was obtained by changing the electrode potential from 0 to 1 V (vs SCE) with a scan rate of 0.10 V/s. The cyclic voltammetry curve of sample was measured in the electrode potential range of −1 to 1 V (vs SCE) at a scan rate of 0.10 V/s. The Tafel polarization curve was measured by changing the electrode potential from 0 to 0.80 V (vs SCE) with a scan rate of 0.01 V/s.

2.5 Analytical methods

The concentration of total iron ions in the filtrate was determined by ICP-OES (PE Optima 8300DV). The concentration of sulfate ions in the filtrate was determined by the barium sulfate turbidimetric method. The pH and E_h were measured with a pH-meter (Lei-ci pHS-2F). Sample was characterized by an X-ray diffractometer (D/MAX-RB) and a scanning electron microscope (SSX−550). The pyrite surface composition after fungal treatment was determined by an X-ray photoelectron spectrometer (XPS) (ESCALAB250). The C 1s peak of adventitious carbon (E_B=284.60 eV) was used for the spectral calibration as an internal standard. All absorbance measurements were conducted with a Double-beam UV-Vis spectrophotometer (Persee TU−190). The concentration of organic acids was determined using high performance liquid chromatography (HPLC) (Agilent 1100). The external standard method was used to quantify organic acids. The pyrite residue with biomass was dried at 80 °C for 24 h, cooled and weighed in a desiccator. Thereafter, the pyrite residues were ashed at 500 °C for 4 h. The mass change occurring due to heating from 80 to 500 °C was used to calculate the fungal biomass [24]. A CHI600E electrochemical workstation was used to perform the electrochemical measurement and analysis. The exposed face of electrode was polished in order to start each experiment with a fresh surface.

3 Results and discussion

3.1 Fungal dissolution of pyrite

Figure 1 presents the contents of dissolved iron and sulfur from pyrite in the systems with and without *P. chrysosporium*. Figure 2 compares pH and E_h during dissolving pyrite with and without *P. chrysosporium*. 0.60% iron and 7% sulfur were dissolved from pyrite in the system without fungi. And pH decreased from 5 to

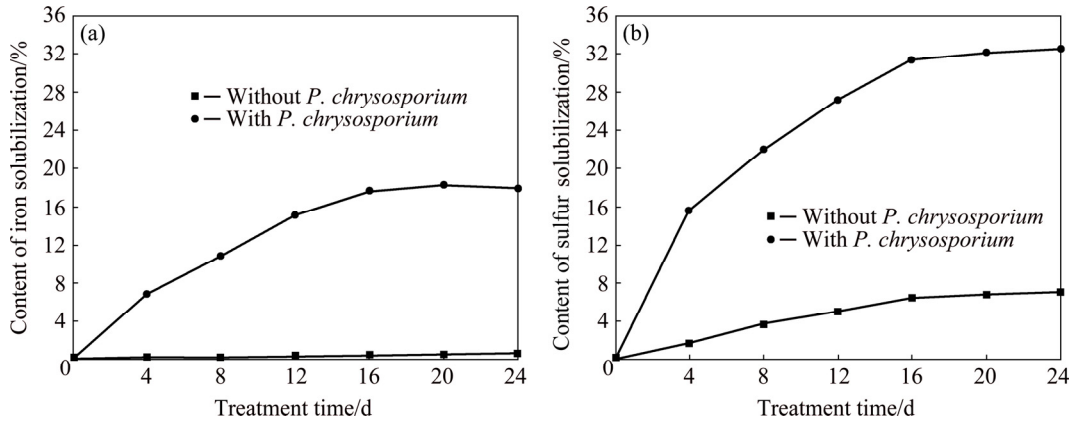

Fig. 1 Dissolved contents of iron (a) and sulfur (b) in systems without and with *P. chrysosporium*

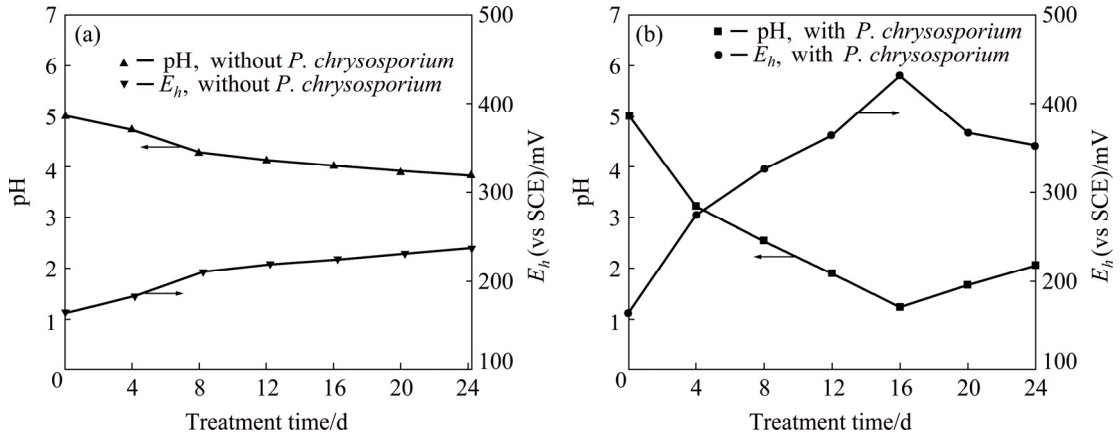

Fig. 2 Changes of pH and E_h in systems without (a) and with (b) *P. chrysosporium*

3.90, while E_h increased from 164 to 237 mV (vs SCE). These changes are attributed to the consumption of dissolved oxygen as shown in Eq. (1). The dissolution data, which were obtained from the interaction of the nitrogen limited medium and pyrite under vacuum condition, are not shown due to the negligible degradation.

$$2FeS_2+7O_2+2H_2O \rightarrow 2Fe^{2+}+4SO_4^{2-}+4H^+ \quad (1)$$

The dissolved contents of iron and sulfur were 18% and 33% in the system with fungi, respectively. The results indicate that *P. chrysosporium* can improve the dissolution of pyrite. In the fungal pure culture system without pyrite, pH decreased to a minimum of 3.80 at day 12, and then increased to 4.30 at day 24. In the fungal system, pH decreased at the beginning, but 16 days later, it rose again to 2.10 at day 24. Compared with the systems without fungi and the fungal pure culture, pH decreased more in the fungal system. These indicate that the fungal dissolution of pyrite is accompanied by the production of organic acids, carbonic acid and sulfuric acid. Organic acids and carbon dioxide are generated by the fungal metabolism, and carbon dioxide reacts with water to form carbonic acid. Sulfuric acid is from the oxidation of pyrite. The slight increase of pH was probably the result of the consumption of organic acids and the generation of nitrogenous bases. In summary, pH variation of the fungal system is probably due to the combined effect of organic acids, carbonic acid, sulfuric acid and nitrogenous bases. E_h initially increased and then decreased as shown in Fig. 2(b). After 16 d of fungal treatment, E_h increased from 164 to 431 mV (vs SCE), which was attributed to the dissolution of pyrite. E_h decreased 16 d later which was probably due to the pH increase and the sediments generation.

Figure 3(a) shows the change of the biomass dry mass and the enzyme activity during 24 d incubation. The fungal biomass increased to the maximum of 1.98 g/L at day 12, followed by the slight decrease and finally remained constant at about 1.40 g/L. MnP activity increased drastically to the maximum of 316 U/L within 4 d, and then remain undetectable after 20 d. Lac activity kept rising till day 8, but subsequently decreased to 0 U/L at day 16. LiP activity increased to the maximum value of 95 U/L at day 8, and then decreased to 0 U/L at day 16.

Organic acids such as oxalic acid, gluconic acid and citric acid were produced with the consumption of the primary carbon source. Figure 3(b) shows change of the concentration of organic acids in the fungal system. The concentrations of oxalic acid and gluconic acid increased significantly at the beginning. The concentration of oxalic acid increased till day 12 and reached the maximum

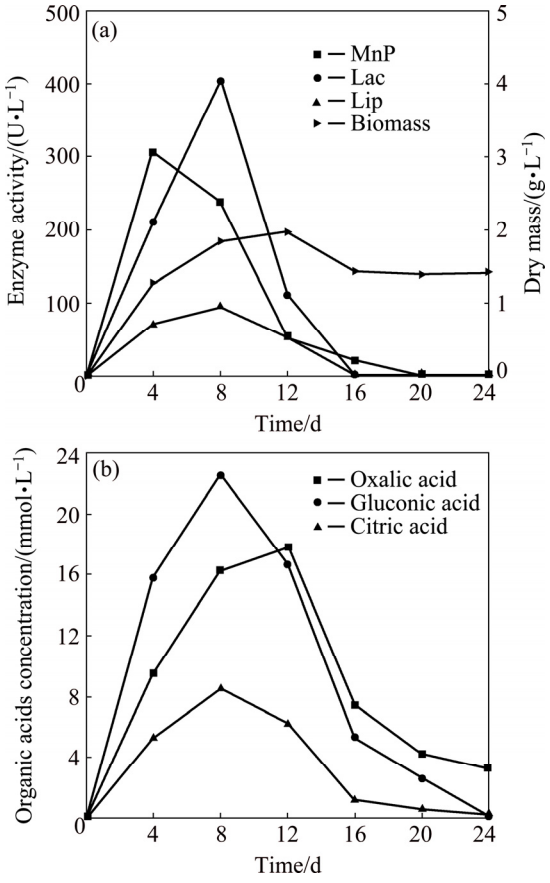

Fig. 3 Changes of fungal biomass and enzyme activity (a) as well as concentration of organic acids (b) in fungal system

of 17.80 mmol/L, and kept decreasing to 3.30 mmol/L at day 24. The concentrations of gluconic acid and citric acid increased to the maximum of 22 mmol/L and 8.60 mmol/L at day 8. Furthermore, it can be concluded that gluconic acid and oxalic acid are the important organic acids which are involved in the dissolution of pyrite. The concentration of organic acids had the positive correlation with the fungal biomass and the enzyme activity, but had negative correlation with pH as shown in Figs. 2 and 3. The dissolution amount of pyrite increased with the increase of the concentration of organic acids and the enzyme activity, as shown in Figs. 1 and 3. Organic acids and enzymes play a direct and important role in the fungal dissolution of pyrite process. When the fungal growth is inhibited by the lower pH as shown in Figs. 1, 2(b) and 3(a), the biomass started to decrease and the dissolution amount of pyrite declined.

3.2 SEM−EDS analysis

The surface morphologies of pyrite are shown in Fig. 4 before and after treatment with *P. chrysosporium*. The surface of original pyrite is mostly clean and with the metallic luster (Fig. 4(a)). The signs of corrosion and precipitates appear on the pyrite surface after treatment

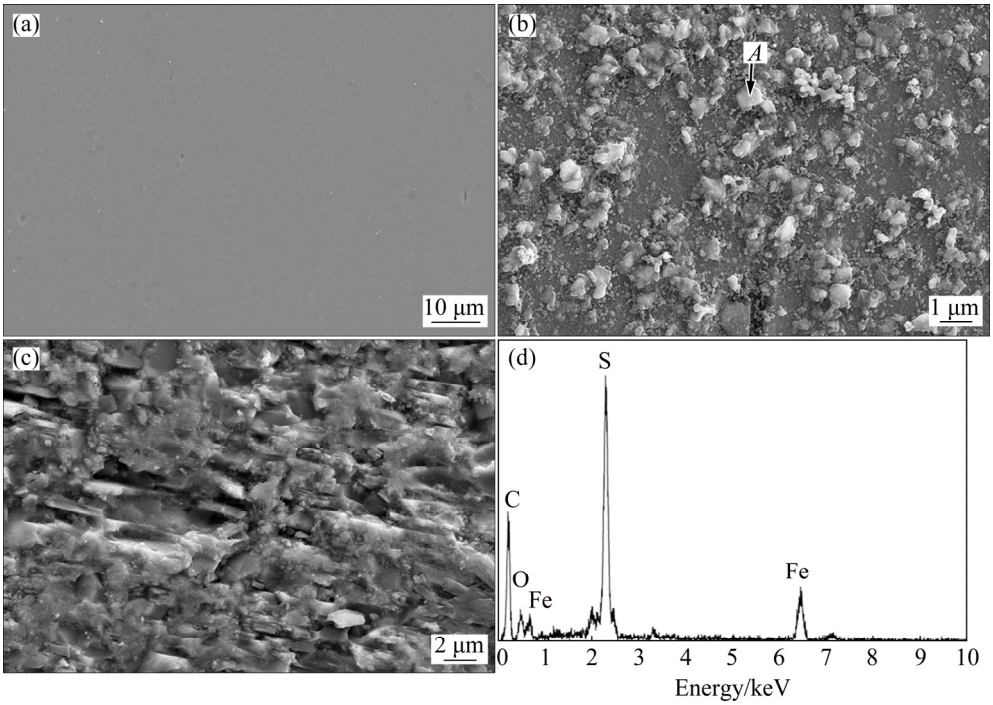

Fig. 4 SEM images of pyrite after treatment for 0 d (a), 12 d (b) and 24 d (c) with *P. chrysosporium*, and EDS analysis of point *A* (d)

for 12 d (Fig. 4(b)). The pyrite surface had been seriously corroded after treatment for 24 d (Fig. 4(c)). Figure 4(d) shows the EDS analysis of point *A* in Fig. 4(b). The presence of element oxygen indicated that pyrite had been oxidized. The existence of element carbon indicated that the precipitates contained biomass, most likely mycelia. The molar ratio of iron to sulfur is 1:2 in pyrite, but changed into 1:3.60 in the filtrate, which is attributed to the formation of iron precipitates.

3.3 XRD analysis

The XRD pattern of the fungal dissolving residue at day 12 is shown in Fig. 5. The XRD pattern indicated that iron oxy-hydroxide (FeO(OH)) and elemental sulfur (S^0) were formed on the pyrite surface. Other ferric precipitates could not be detected, probably, because they are below the detection limit. The surface oxidized layer, which is formed by the above-mentioned precipitates, could act as the diffusion barrier and prevent the further dissolution of pyrite [6,25].

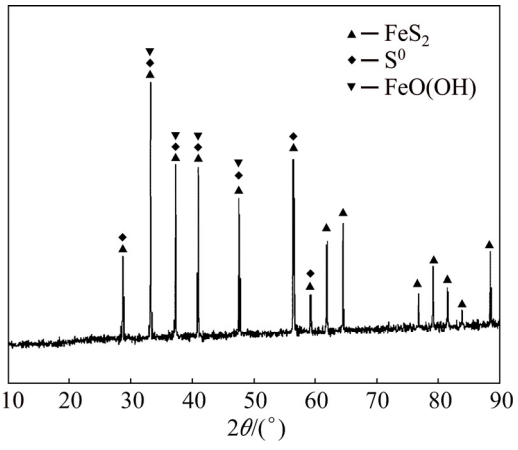

Fig. 5 XRD pattern of pyrite after fungal treatment for 12 d

3.4 XPS analysis

Fe $2p_{3/2}$, S 2p and O 1s spectra of pyrite after fungal treatment for 12 d are presented in Fig. 6. The Fe $2p_{3/2}$ spectrum of pyrite had a major peak near 708 eV. Three peaks at 711.69, 708.32 and 706.86 eV were fitted to the Fe $2p_{3/2}$ spectrum. Peak 1 at 711.69 eV could be interpreted as the ferric ions (Fe^{3+}) of iron oxy-hydroxide and oxides [26,27]. This indicated that a part of ferrous irons of pyrite were oxidized to ferric ions. Peak 2 at 708.32 eV was assigned to (Fe^{2+})—O— and (Fe^{3+})—S— bonds [26,28]. Peak 3 at 706.86 eV represented (Fe^{2+})—S— bonds, which was derived possibly from partially oxidized or unoxidized pyrite beneath the oxidized layer [26].

A strong SO_4^{2-} signal appeared near 169 eV in the S 2p spectrum. The presence of (Fe^{3+})—S— and SO_4^{2-} peaks indicated that $Fe_2(SO_4)_3$ and H_2SO_4 were generated during the fungal dissolution of pyrite. The production of H_2SO_4 contributed to the decrease of pH as shown in Fig. 2. Under the acidic condition the crystal lattice of pyrite was destroyed by the attack of Fe^{3+} [4,29]. Peak 2 at 163.70 eV was assigned to S^0, which correlated with the result obtained by XRD analysis (Fig. 5). Peak 3 at 162.31 eV could be attributed to polysulfide species (S_2^{2-}) [28].

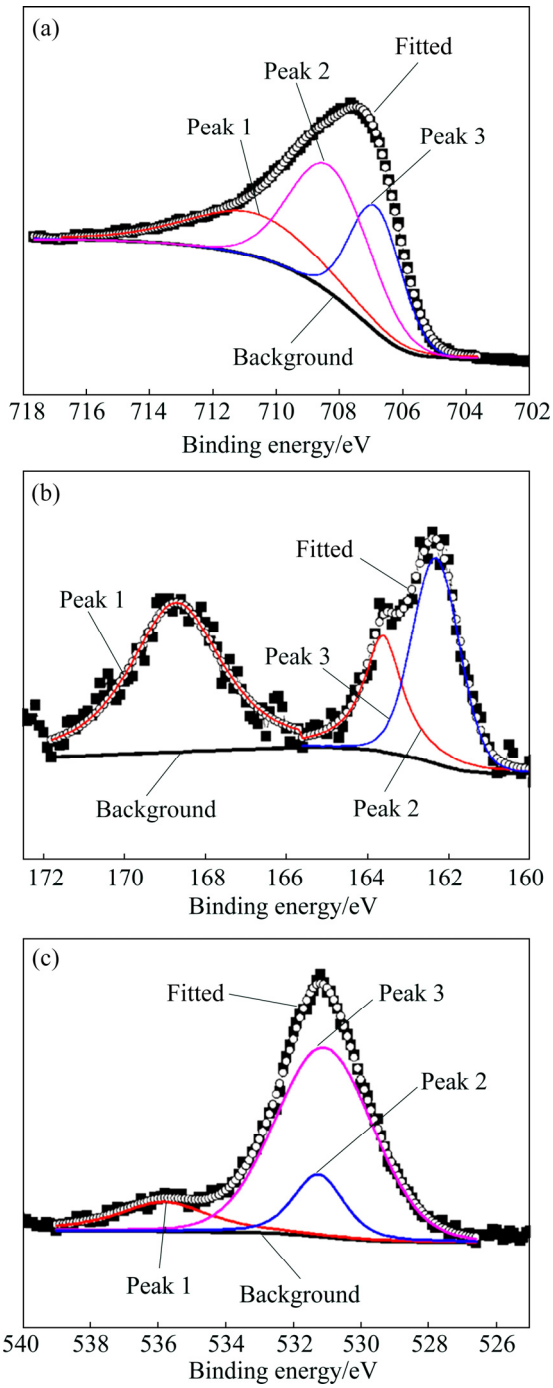

Fig. 6 Fe $2p_{3/2}$ (a), S 2p (b) and O 1s (c) spectra of pyrite surface after fungal treatment for 12 d

The O ls spectrum revealed three peaks at 535.80 eV (adsorbed water), 531 eV (oxides) and 531.30 eV (hydroxide), respectively. The area ratio of oxides (O^{2-}) to hydroxides (OH^-) was about 5:1, indicating that the content of the oxides was higher than hydroxides. Fe $2p_{3/2}$, S 2p and O 1s spectra demonstrated that the oxidized layer of pyrite surface consisted of iron oxides, iron oxy-hydroxides, iron hydroxides, ferric sulfate and elemental sulfur.

3.5 Electrochemical characteristic of pyrite

3.5.1 Steady-state polarization curve

Figure 7 shows steady-state polarization curves of pyrite electrode in the systems without and with *P. chrysosporium*. The polarization current density remained constant, when the applied potential swept from 0 to 0.80 V (vs SCE) and to 0.20 V (vs SCE) without and with fungi, respectively. This indicated that the electrode surface was passivated at the initial stage of scanning. The potentials and the current densities at 0.80 and 0.20 V (vs SCE) were the pitting potential and the pitting current density of the systems without and with fungi. The pitting current densities of two systems exhibited negligible differences. However, the pitting potentials of two systems had significant difference. The pitting potentials of the systems without and with fungi were 0.80 and 0.20 V (vs SCE), respectively. When the scanning potential was higher than the pitting potential, the current density increased due to the break-down of the passive film [30]. The current density of pyrite electrode increased rapidly from 0 to 8.40 mA in the system with fungi, but the increase was not significant in the sterile system. The results indicated that *P. chrysosporium* could significantly accelerate the dissolution of pyrite by decreasing the pitting potential and increasing the polarization current.

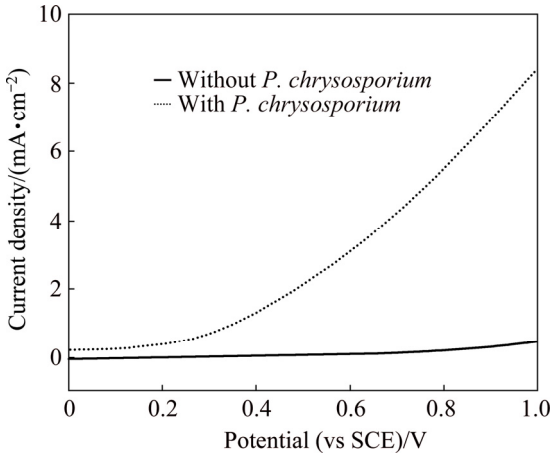

Fig. 7 Steady-state polarization curves of pyrite electrode in systems without and with *P. chrysosporium*

3.5.2 Cyclic voltammetry curve

Figure 8 shows cyclic voltammetry curves of pyrite electrode in the systems without and with fungi. Compared with the sterile system, the peak current of the fungal system significantly increased. Fungi could reduce the initial oxidation potential of pyrite from 0.75 to 0.10 V (vs SCE). In the fungal system, three oxidation peaks appeared during the anodic scan. Three oxidation peaks located at 0.10, 0.50 and 0.75 V (vs SCE), respectively. Peak A_1 was correlated with the oxidation of S_2^{2-} and the dissolution of Fe^{2+} from pyrite as shown in

Eq. (2). Peak A_2 corresponded to the conversion of Fe^{2+} to Fe^{3+} according to Eq. (3). However, this peak was not found in the sterile system, which was mainly attributed to the lack of strong oxidation environment. When the scan potential above 0.75 V (vs SCE) was reached, S^0 was oxidized to SO_4^{2-}, which corresponded to peak A_3. During the cathodic scan, two peaks appeared at about 0.10 and −0.40 V (vs SCE), respectively. Peak C_1 was related to the reduction of Fe^{3+}. Peak C_2 was assigned to the reduction of FeS_2 and S^0 as shown in Eqs. (4) and (5) [30,31].

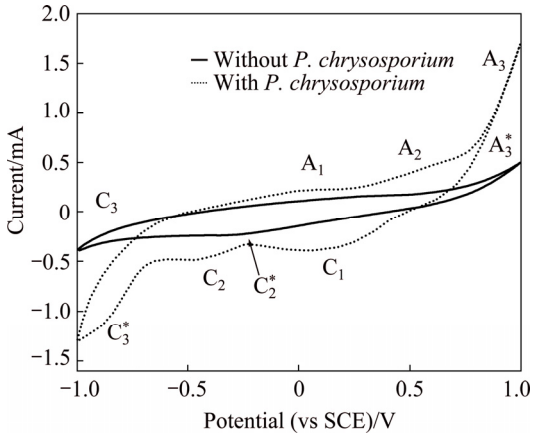

Fig. 8 Cyclic voltammetry curves of pyrite electrode in systems without and with *P. chrysosporium*

In the sterile system, a weak oxidation peak A_3* was observed at 0.75 V (vs SCE). Peak A_3* was attributed to the oxidation of dissolved oxygen as shown in Eq. (1). Peak C_2* at −0.30 V (vs SCE) was analogous to the peak C_2. Peaks C_3 and C_3* were the hydrogen evolution peak from the reduction of water. The intensity of peak C_3 was higher than peak C_3*, which indicated that fungi promoted the hydrogen evolution.

$$FeS_2 \rightarrow Fe^{2+}+2S^0+2e \quad (2)$$

$$Fe^{2+} \xleftarrow{P.\ chrysosporium} Fe^{3+}+e \quad (3)$$

$$FeS_2+2H^++2e \rightarrow FeS+H_2S \quad (4)$$

$$S^0+2H^++2e \rightarrow H_2S \quad (5)$$

3.5.3 Tafel polarization curve

Figure 9 shows Tafel polarization curves of pyrite electrode in the systems without and with fungi. The electrochemical polarization parameters: corrosion potential (φ_{corr}), corrosion current density (J_{corr}), anode slope (b_a), cathode slope (b_c) and polarization resistance (R_p) are listed in Table 1. A comparison revealed that φ_{corr} and J_{corr} increased significantly in the fungal system. b_c of pyrite electrode in the fungal system was higher than that of the sterile system, but b_a was lower than former. The values of b_a and b_c are $2.303RT/(n_\beta F)$ and $2.303RT/(n_\alpha F)$, respectively, where n_α and n_β are the electron transfer coefficients. This indicated that n_α decreased, whereas n_β increased. The results indicated that *P. chrysosporium* could accelerate the dissolution of pyrite by inhibiting the cathodic reaction and promoting the anodic reaction. Also, R_p reduced in the presence of *P. chrysosporium*, their corrosive ability was further proved.

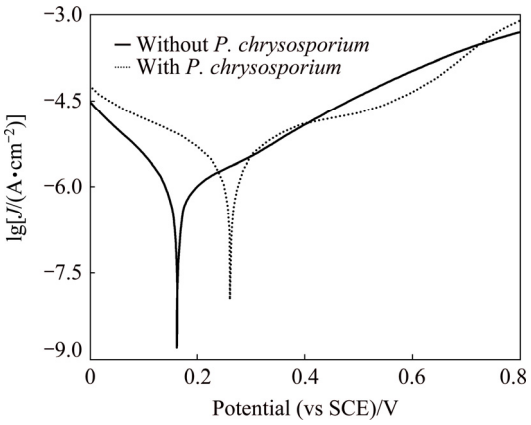

Fig. 9 Tafel polarization curves of pyrite electrode in systems without and with *P. chrysosporium*

4 Mechanism of pyrite with *P. chrysosporium*

The dissolution of pyrite with *P. chrysosporium* is the combined action of hydrogen peroxide, enzymes, ferric iron and organic acids.

1) The lignin degradation enzyme system mainly consists of the hydrogen peroxide-producing enzyme and the lignin-oxidase enzyme systems. Hydrogen peroxide (H_2O_2), produced by the hydrogen peroxide synthetase, activates peroxidase and triggers the lignin degradation. H_2O_2 participates in the oxidative corrosion of pyrite are shown by Eq. (6) [6,32,33].

$$2FeS_2+15H_2O_2 \rightarrow 2Fe^{3+}+4SO_4^{2-}+14H_2O+2H^+ \quad (6)$$

2) The fungal dissolution of pyrite is probably the

Table 1 Electrochemical polarization parameters of pyrite electrode in systems without and with *P. chrysosporium*

System	φ_{corr}(SCE)/mV	J_{corr}/(mA·cm^{-2})	b_c/(mV·decade^{-1})	b_a/(mV·decade^{-1})	R_p/(Ω·cm^{-2})
Without fungi	163	0.001	114.78	222.47	2.67×10^4
With fungi	246	0.002	179.47	193.20	1.82×10^4

result of the chain reactions based on free radicals by the lignin degradation enzyme system. The specific mechanism is shown in Fig. 10. Firstly, the enzyme−P(Fe^{3+}) loses two electrons by the reaction with H_2O_2 and forms the positive charged free radical —P(O═Fe^{4+}•). Secondly, P(O═Fe^{4+}•) reacts with FeS_2, which results in the electron transfer from FeS_2 to P(O═Fe^{4+}•) and forms S^0 and free radical FeS^+•. The free radical P(O═Fe^{4+}) returns to the initial status by the reaction with FeS_2, S^0, FeS^+• and Fe^{2+}, and then the next cycle starts. The generated free radicals can attack the chemical bonds of FeS_2.

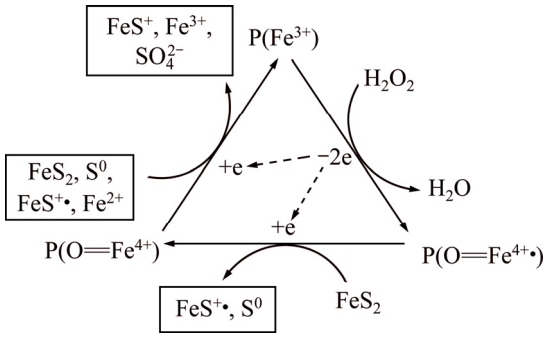

Fig. 10 Enzyme-free radicals mechanism of pyrite with *P. chrysosporium* [15]

3) The activity of *P. chrysosporium* can affect the production of organic acids and the enzyme activity. After 12 d, the concentration of organic acids and the enzyme activity all took on the evident downtrend with the decrease of the fungal biomass (Fig. 3). However, the dissolved amounts of iron and sulfur still increased until 16 d. It is well known that the precipitation of ferric iron is formed when pH is above 2.60. Furthermore, pH of the fungal system was below 2.60 from 8 to 24 d. Therefore, the attack of ferric iron probably plays an important role in the middle and later periods. Moreover, the dissolution of pyrite with organic acids is mainly by acidolysis and complexolysis [10,13,34].

5 Conclusions

1) *P. chrysosporium* is able to dissolve pyrite. After 24 d treatment with *P. chrysosporium*, 18% of iron and 33% of sulfur were dissolved from pyrite.

2) The oxidization layer on the pyrite surface probably consists of iron oxides, iron hydroxides, ferric sulfate, elemental sulfur and mycelia.

3) *P. chrysosporium* can accelerate the transformation process of Fe^{2+} to Fe^{3+} and S^- to SO_4^{2-} by decreasing pitting potential and polarization resistance plus increasing polarization current, corrosion potential and corrosion current density.

4) The synergistic effects of enzyme-free radicals, hydrogen peroxide, ferric iron ions and organic acids result in the dissolution of pyrite. Enzymes break the chemical bonds of pyrite with the generated free radicals. Organic acids probably dissolve pyrite by acidolysis and complexolysis.

5) Among them, the enzyme-free radicals and hydrogen peroxide are considered to be the important factors during the fungal dissolution of pyrite.

References

[1] REES K L, van DEVENTER J S J. Preg-robbing phenomena in the cyanidation of sulphide gold ores [J]. Hydrometallurgy, 2000, 58(1): 61−80.

[2] BAS A D, ALTINKAYA P, YAZICI E Y, DEVECI H. Preg-robbing potential of sulphide-bearing gold ores [C]//ÖZDAĞ H, BOZKURT V, İPEK H, BİLİR K. Proceedings of the XIII International Mineral Processing Symposium. Bodrum, Turkey: Department of Mining Engineering, Eskişehir Osmangazi University, 2012: 613−618.

[3] CHRYSSOULIS S L. Gold "preg-robbing" by pyrite: Natural and process induced [C]//NEGERI T, WILSON J, CHEVALIER G. Proceedings of the 29th Annual Meeting of the Canadian Mineral Processors. Ottawa, Canada: Canadian Institute of Mining, 1997: 1−12.

[4] SAND W, GEHRKE T, JOZSA P G, SCHIPPERS A. (Bio)chemistry of bacterial leaching—direct vs. indirect bioleaching [J]. Hydrometallurgy, 2001, 59(2−3): 159−175.

[5] YANG Hong-ying, GONG En-pu, YANG Li-li, WANG Da-wen. Chemical behaviors of different arsenic-bearing sulphides bio-oxidated by thermophilic bacteria [J]. Transactions of Nonferrous Metals Society of China, 2005, 15(3): 648−652.

[6] OFORI-SARPONG G, OSSEO-ASARE K, TIEN M. Fungal pretreatment of sulfides in refractory gold ores [J]. Minerals Engineering, 2011, 24(6): 499−504.

[7] AMANKWAH R K, YEN W T, RAMSAY J A. A two-stage bacterial pretreatment process for double refractory gold ores [J]. Minerals Engineering, 2005, 18(1): 103−108.

[8] PYKE B L, JOHNSTON R F, BROOKS P. The characterization and behavior of carbonaceous material in a refractory gold bearing ore [J]. Minerals Engineering, 1999, 12(8): 851−862.

[9] BRIERLEY J A, KULPA C F. Microbial consortium treatment of refractory precious metal ores: U.S. Patent, 5,127,942 [P]. 1992-07-07.

[10] IIYAS S, CHI Ru-an, LEE J C, BHATTI H N. One step bioleaching of sulphide ore with low concentration of arsenic by *Aspergillus niger* and taguchi orthogonal array optimization [J]. Chinese Journal of Chemical Engineering, 2012, 20(5): 923−929.

[11] WU H Y, TING Yen-peng. Metal extraction from municipal solid waste (MSW) incinerator flyash—Chemical leaching and fungal bioleaching [J]. Enzyme and Microbial Technology, 2006, 38(6): 839−847.

[12] BISWAS S, BHATTACHARJEE K. Fungal assisted bioleaching process optimization and kinetics: Scenario for Ni and Co recovery from a lateritic chromite overburden [J]. Separation and Purification Technology, 2014, 135: 100−109.

[13] QU Yang, LIAN Bin, MO Bin-bin, LIU Cong-qiang. Bioleaching of heavy metals from red mud using *Aspergillus niger* [J]. Hydrometallurgy, 2013, 136: 71−77.

[14] DENG Xin-hui, CHAI Li-yuan, YANG Zhi-hui, TANG Chong-jian, WANG Yang-yang, SHI Yan. Bioleaching mechanism of heavy metals in the mixture of contaminated soil and slag by using indigenous *Penicillium chrysogenum* strain F1 [J]. Journal of Hazardous Materials, 2013, 248−249: 107−114.

[15] OFORI-SARPONG G, OSSEO-ASARE K, TIEN M. Myco-hydrometallurgy: Biotransformation of double refractory gold ores by the fungus, *Phanerochaete chrysosporium* [J]. Hydrometallurgy, 2013, 137: 38−44.
[16] OFORI-SARPONG G, TIEN M, OSSEO-ASARE K. Myco-hydrometallurgy: Coal model for potential reduction of preg-robbing capacity of carbonaceous gold ores using the fungus, *Phanerochaete chrysosporium* [J]. Hydrometallurgy, 2010, 102 (1−4): 66−72.
[17] LIU Qian, YANG Hong-ying, TONG Lin-lin. Influence of *Phanerochaete chrysosporium* on degradation and preg-robbing of activated carbon [J]. Transactions of Nonferrous Metals Society of China, 2014, 24(6): 1905−1911.
[18] AYTAR P, ŞAM M, ÇABUK A. Microbial desulphurization of Turkish lignites by white rot fungi [J]. Energy and Fuels, 2008, 22(2): 1196−1199.
[19] LIU Qian, YANG Hong-ying, QIAO Li-li. Biotransformation of arsenopyrite by *Phanerochaete chrysosporium* [J]. Advanced Materials Research, 2013, 825: 309−313.
[20] SATO S, LIU Feng, KOC H, TIEN M. Expression analysis of extracellular proteins from *Phanerochaete chrysosporium* grown on different liquid and solid substrates [J]. Microbiology, 2007, 153(9): 3023−3033.
[21] TIEN M, KIRK T K. Lignin Peroxidase of *Phanerochaete chrysosporium* [J]. Methods in Enzymology, 1988, 161: 238−249.
[22] HOFRICHTER M, FRITSCHE W. Depolymerization of low-rank coal by extracellular fungal enzyme systems. II. The ligninolytic enzymes of the coal-humic-acid-depolymerizing fungus *Nematoloma frowardii* bl9 [J]. Applied Microbiology and Biotechnology, 1997, 47(4): 419−424.
[23] AYTAR P, GEDIKLI S, ŞAM M, ÜNAL A, ÇABUK A, KOLANKAYA N, YÜRÜM A. Desulphurization of some low-rank Turkish lignites with crude laccase produced from *Trametes versicolor* ATCC 200801 [J]. Fuel Processing Technology, 2011, 92(1): 71−76.
[24] AUNG K M, TING Y P. Bioleaching of spent fluid catalytic cracking catalyst using *Aspergillus niger* [J]. Journal of Biotechnology, 2005, 116(2): 159−170.
[25] MOUSAVI S M, YAGHMAEI S, SALIMI F, JAFARI A. Influence of process variables on biooxidation of ferrous sulfate by an indigenous *Acidithiobacillus ferrooxidans*. Part I: Flask experiments [J]. Fuel, 2006, 85(17−18): 2555−2560.
[26] NESBITT H W, MUIR I J, PRARR A R. Oxidation of arsenopyrite by air and air-saturated, distilled water, and implications for mechanism of oxidation [J]. Geochimica Et Cosmochimica Acta, 1995, 59(9): 1773−1786.
[27] FANTAUZZI M, LICHERI C, ATZEI D, LOI G, ELSENER B, ROSSI G, ROSSI A. Arsenopyrite and pyrite bioleaching: Evidence from XPS, XRD and ICP techniques [J]. Analytical and Bioanalytical Chemistry, 2011, 401(7): 2237−2248.
[28] NESBITT H W, MUIR I J. Oxidation states and speciation of secondary products on pyrite and arsenopyrite reacted with mine waste waters and air [J]. Mineralogy and Petrology, 1998, 62(1−2): 123−144.
[29] TRIBUTSCH H. Direct versus indirect bioleaching [J]. Hydrometallurgy, 2001, 59(2−3): 177−185.
[30] GU Guo-hua, SUN Xiao-jun, HU Ke-ting, LI Jian-hua, QIU Guan-zhou. Electrochemical oxidation behavior of pyrite bioleaching by *Acidthiobacillus ferrooxidans* [J]. Transactions of Nonferrous Metals Society of China, 2012, 22(5): 1250−1254.
[31] GIANNETTI B F, BONILLA S H, ZINOLA C F, RABÓCZKAY T. A study of the main oxidation products of natural pyrite by voltammetric and photoelectron chemical responses [J]. Hydrometallurgy, 2001, 60(1): 41−53.
[32] ANTONIJEVIĆ M M, DIMITRIJEVIĆ M, JANKOVIĆ Z. Leaching of pyrite with hydrogen peroxide in sulphuric acid [J]. Hydrometallurgy, 1997, 46(1−2): 71−83.
[33] JENNINGS S R, DOLLHOPF D J, INSKEEP W P. Acid production from sulfide minerals using hydrogen peroxide weathering [J]. Applied Geochemistry, 2000, 15(2): 235−243.
[34] BURGSTALLER W, SCHINNER F. Leaching of metals with fungi [J]. Journal of Biotechnology, 1993, 27(2): 91−116.

黄孢原毛平革菌对黄铁矿的溶解作用

杨洪英[1]，刘 倩[1,2]，陈国宝[1]，佟琳琳[1]，Auwalu ALI[1]

1. 东北大学 冶金学院，沈阳 110819；
2. 上海第二工业大学 上海电子废弃物资源化协同创新中心，上海 201209

摘 要：研究黄孢原毛平革菌(*Phanerochaete chrysosporium*)对黄铁矿的溶解。经该菌作用后，黄铁矿中铁和硫的溶解量分别为18%和33%。在黄铁矿表面形成的氧化层可能由铁的氧化物、FeOOH、硫酸铁、元素硫及菌丝体组成。研究黄铁矿在无菌和有菌体系的电化学特征。*P. chrysosporium* 通过降低点蚀电位和极化电阻，提高极化电流、腐蚀电位和腐蚀电流密度的方式促进黄铁矿溶解。*Phanerochaete chrysosporium* 对硫化物的溶解是酶、H_2O_2、Fe^{3+}和有机酸联合作用的结果。酶通过自由基攻击化学键，有机酸通过酸解和络合作用溶解黄铁矿。酶和 H_2O_2 在黄铁矿溶解过程中发挥了重要作用。

关键词：黄孢原毛平革菌；黄铁矿；生物溶解；卡林型金矿；电化学

(Edited by Xiang-qun LI)